

Mixed external cavity mode dynamics in a semiconductor laser

David W. Sukow, Michael C. Hegg, and Jennifer L. Wright

Department of Physics and Engineering, Washington and Lee University, Lexington, Virginia 24450

Athanasios Gavrielides

Air Force Research Laboratories, Directed Energy Directorate/DELO, 3550 Aberdeen Avenue SE, Kirtland Air Force Base, New Mexico 87117

Received November 26, 2001

We observe experimentally and numerically novel mixed-mode dynamic states of a diode laser subject to two delayed optical feedbacks. These states have been proposed and analyzed within the framework of the Lang-Kobayashi single-feedback model. Such states are combinations of two distinct external cavity modes and can be identified through a characteristic sequence of a Hopf bifurcation followed by a secondary quasi-periodic bifurcation. We present experimental and numerical results that demonstrate such sequences.

© 2002 Optical Society of America

OCIS codes: 140.1540, 140.2020, 140.5960, 190.3100.

Diode lasers subjected to weak or moderate optical feedback exhibit a large range of instabilities. The resulting pulsating optical intensities arise because of a combination of factors: the large size of the optical feedback delay relative to the photon lifetime and the influence of the large phase-amplitude coupling present in diode lasers. These and other factors define the properties of the external cavity modes (ECMs) created by the feedback, which in turn strongly influence the dynamic instabilities displayed by such a laser.

Recently, Erneux *et al.*¹ explored the dynamics that can arise in systems in which the laser is subjected to delayed optical feedback from two distant reflectors. Some of this research was motivated by a desire to control the unstable dynamics induced by one feedback by means of a second, well-chosen feedback.² However, novel dynamic states of interest in their own right have also been observed in dual-feedback systems. Notably, in past experimental work what appear to be stable high-frequency oscillations in optical spectra were observed.³ In view of the theoretical work by Erneux *et al.*,¹ it was suggested that such oscillations could arise from the beating between two different ECMs. This finding has provoked a new interest in such regimes, first studied for lasers with single optical feedback from a short external cavity.^{4,5} To understand these states is important from the standpoint of control, in that they tend to lie between regions of stability in a bifurcation cascade. They could also prove useful as a novel, all-optical source of radio-frequency oscillations.

Theoretical advances suggest that the high-frequency oscillations arise not from the well-known mechanism of a Hopf bifurcation but from a novel Hopf bifurcation in which the time-periodic solutions are a combination of two distinct ECMs: a mode and an antimode that appear close to a degenerate point at which the mode's intensity is equal to that of the antimode. The oscillation frequency is then equal to the frequency difference between the two ECMs. A clear dynamic signature identifies the dynamics that

originate from such a mixed-mode state: beginning with stable emission on one ECM, the laser undergoes a Hopf bifurcation to periodicity, followed by a secondary quasi-periodic bifurcation, concluding with restabilization on a new ECM. As will be shown in this Letter, the same sequence reveals a mixed-mode state in two-cavity systems as well. We focus on this particular feature of the two-cavity system.

The experiment uses a temperature-stabilized diode laser (SDL 5401-G1) that emits at a nominal wavelength of $\lambda = 808$ nm and has a solitary threshold of 24.89 mA. For all the experimental results described in this paper, the pump current is 24.62 mA. As illustrated in Fig. 1, the laser beam passes through a collimating lens (CL) and a polarizing beam splitter (PBS) whose transmission axis is parallel to the polarization axis of the laser beam. The reflected beam of the PBS leads out of the experimental system (dashed box) where a lens focuses the beam onto a photodetector [(PD) Hamamatsu C4258-01, 8.75-GHz bandwidth]. The photodetector signal goes to an amplifier [(AMP) 23-dB gain] whose output then feeds into a digital storage oscilloscope [(DSO) LeCroy 9384M, 1-GHz bandwidth] and a

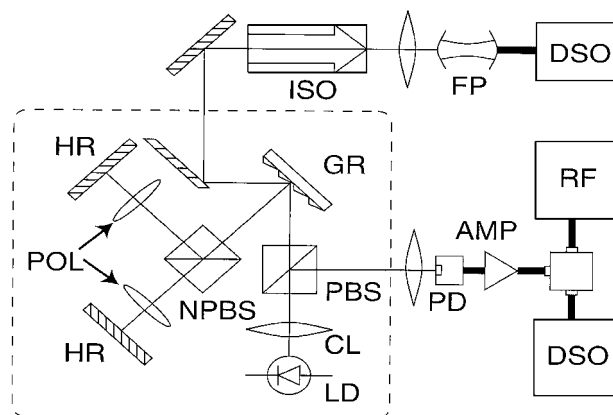


Fig. 1. Experimental schematic diagram; see text for definitions.

radio-frequency spectrum analyzer [(RF) Agilent E4405 B]. The transmitted beam of the PBS strikes a diffraction grating (GR). The zeroth-order beam of the diffraction grating travels to a Fabry–Perot (FP) interferometer optical spectrum analyzer (OSA) Newport SR-240C, 1100-GHz free spectral range, >13,000 finesse]; the Faraday isolator (ISO, >36-dB isolation) protects the system from unwanted feedback from the optical spectrum analyzer. The first-order beam of the grating leads to two external cavities, which were formed by a nonpolarizing beam splitter (NPBS) and two 99% reflective mirrors. The grating allows frequency selectivity of the optical feedback, narrowing the cavity bandwidth to ~ 50 GHz. Both cavities are aligned to force the laser to oscillate in the same solitary longitudinal mode. The path lengths of the two cavities are $L_1 = 19$ cm and $L_2 = 16$ cm. Two rotatable polarizers (POL) adjust the feedback strengths of the external cavities, characterized by fractional threshold reductions $\Delta I = (I_{\text{th}} - I)/I_{\text{th}}$. This choice is made to allow easy comparisons between ΔI and the theoretical normalized feedback strengths.

The key experimental data are the optical spectra and the RF spectra presented in Figs. 2 and 3, respectively. Figure 2 displays a progression of optical spectra as feedback from the second cavity increases; successive spectra are offset vertically for clarity. The vertical axis is scaled in normalized units of optical power such that the height of the peak in trace (b) is set to 1. The horizontal axis is the frequency shift as measured relative to the first ECM that becomes active when feedback from the first cavity alone is applied. The initial optical spectrum [Fig. 2, trace (a)] is the reference state, where $\Delta I_2 = 0.00\%$. At this point, the threshold reduction that is due to the first cavity feedback is $\Delta I_1 = 2.40\%$. Three ECMs of the first cavity are active. When the feedback from the second cavity is introduced, with a threshold reduction of $\Delta I_2 = 2.18\%$, the laser stabilizes on one ECM [Fig. 2, trace (b)]. The corresponding RF spectrum [Fig. 3(a)] is flat. The laser then undergoes a Hopf bifurcation to periodicity as ΔI_2 increase to 4.42%. The optical spectrum [Fig. 2, trace (c)] shows a small sideband, indicating that the original signal has acquired another frequency line located 3.78 GHz away. This behavior is confirmed by the RF spectrum [Fig. 3(b)], which clearly shows the high-frequency oscillation associated with the optical spectrum's primary signal and sideband. At $\Delta I_2 = 4.92\%$, the oscillations grow in amplitude and the sideband grows in the optical spectrum [Fig. 2, trace (d)]. When $\Delta I_2 = 4.97\%$, a secondary bifurcation to quasi-periodicity occurs. In the optical spectrum [Fig. 2, trace (e)], small sidebands appear about the main peaks, with the second frequency close to that of the ECM spacing. The RF spectrum [Fig. 3(c)] shows the associated set of frequencies; the narrowness of the lines confirms the interpretation of quasi-periodicity. At $\Delta I_2 = 5.45\%$, the laser moves to a low-frequency fluctuation (LFF) state. The laser oscillates on multiple ECMs [Fig. 2, trace (f)] and the lines in its RF spectrum [Fig. 3(d)] broaden. Time series data (not shown) confirm this identification con-

clusively. As ΔI_2 increases a final time to 5.74%, the laser restabilizes on a different ECM [Fig. 2, trace (g)].

We now turn to a theoretical examination of this problem. The equations and parameters that describe a single-mode diode laser with two external cavities are given fully in Ref. 2. This model is valid for our experiment because other solitary modes of the laser do not contribute meaningfully to the mixed-mode dynamics (as they might in LFF), since the laser never experiences a power dropout during which other modes could grow briefly from spontaneous emission. For a cavity lifetime of $\gamma = 1/\tau_p = 4.2 \times 10^{11} \text{ s}^{-1}$ and from the experimental conditions, we estimate the various parameters in the equations to be $\tau_1 = 533$, $\tau_2 = 450$, $\eta_1 = 0.024$, and $P = -0.011$. We estimate that the laser has a linewidth enhancement factor of $a = 4$, and a ratio of carrier lifetime to photon lifetime of $T = 420$. For all our subsequent results we regard the feedback strength from the second cavity η_2 as our bifurcation parameter and examine the behavior of the laser as η_2 is increased. We arbitrarily fix the feedback phases of the two cavities to be $\omega_0\tau_1 = \omega_0\tau_2 = -1.45$. The relative phase is not determined experimentally and does not affect the calculations and conclusions. Although the exact phases do affect the locations of individual modes in phase space, many crossings of ECM pairs in

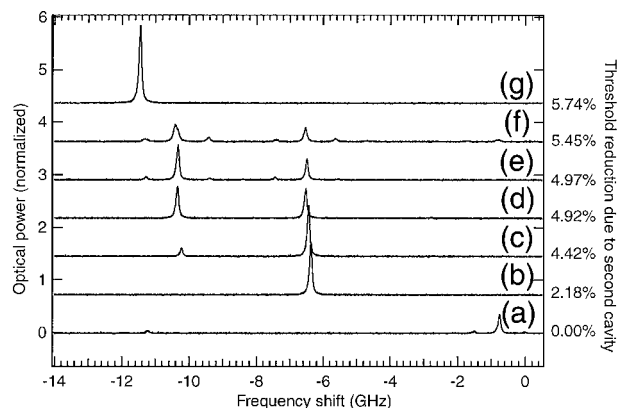


Fig. 2. Experimental optical spectra as a function of ΔI_2 . Threshold reduction from the first cavity is fixed at $\Delta I_1 = 2.40\%$. The laser is stable in traces (b) and (g), periodic in (c) and (d), quasi-periodic in (e), and displays LFF in (f).

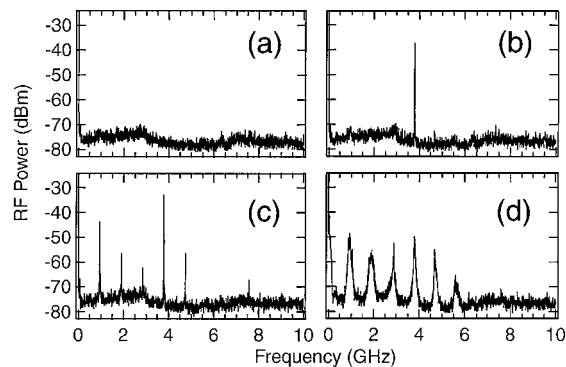


Fig. 3. Experimental RF spectra showing a sequence of dynamics: (a) $\Delta I_2 = 2.18\%$, stable; (b) $\Delta I_2 = 4.42\%$, periodic; (c) $\Delta I_2 = 4.97\%$, quasi-periodic; (d) $\Delta I_2 = 5.45\%$, LFF.

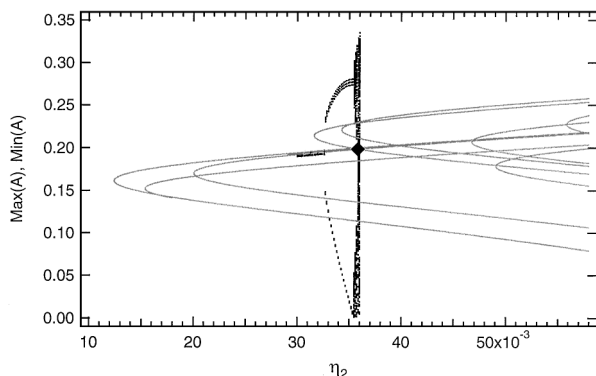


Fig. 4. Analytical and numerical bifurcation diagram. Mode crossing appears at $\eta_2 = 0.036$.

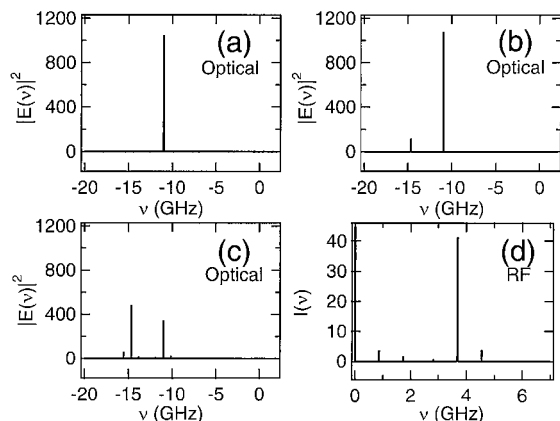


Fig. 5. Numerical optical and RF spectra when $\eta_1 = 0.024$. Optical spectra: (a) $\eta_2 = 0.031$, stable; (b) $\eta_2 = 0.033$, periodic; (c) $\eta_2 = 0.0355$, quasi-periodic. RF spectrum: (d) $\eta_2 = 0.0355$, quasi-periodic.

intensity are possible and therefore, in principle, many mixed-mode solutions can be found.

The effect of the second cavity on the modes of the first cavity and the generation of new modes is seen in Fig. 4, in which the steady-state amplitude is plotted as a function of η_2 , keeping the feedback of the first cavity η_1 fixed at a value of 0.024. Most of the modes of the first cavity survive when the second feedback is introduced; however, some of them annihilate each other and disappear.³ New cavity modes associated with the second cavity appear through saddle-node bifurcations at more negative frequencies. In Fig. 4 we can detect a number of primary mode crossings associated with these new modes. In this case there are not only mode-antimode crossings as was the case in the single cavity, but now primary mode-mode crossings are also possible. We concentrate on the crossing indicated by the diamond at approximately $\eta_2 = 0.036$, which corresponds to the crossing of the mode and not an adjacent antimode. The two modes involved can be inferred by the position of the saddle-node bifurcation in frequency and amplitude space. A numerical bifurcation diagram as a function of η_2 is superimposed on the steady-state solutions near the crossing as shown in Fig. 4. The numerical steady state overlaps the analytical steady state until a Hopf bifurcation occurs just before the ECM crossing, which

is consistent with the analysis and numerical results in Ref. 1. Furthermore, this oscillating state is destabilized by a secondary quasi-periodic bifurcation that leads to LFF.

Next we reproduce a series of numerical optical and RF spectra along this bifurcation diagram for comparison with the experimental sequence. In Fig. 5(a) we show the optical spectra at $\eta_2 = 0.031$, indicating that the laser operates in a steady state located at an external cavity frequency of -11.0 GHz relative to the solitary laser frequency. The RF spectrum (not shown) is flat in this case. Figure 5(b) shows the optical spectrum at $\eta_2 = 0.033$ after the Hopf bifurcation. The optical spectrum has a second frequency appearing at approximately -15 GHz corresponding to the frequency of the second mode. The RF spectrum (not shown) displays a peak located near 3.7 GHz, the beat frequency of the two modes, which is close to four times the external cavity frequency and is in good agreement with that measured experimentally.

This sequence of bifurcations must continue with a quasi-periodic bifurcation because the Hopf branch connects a stable node to an unstable saddle. Therefore the Hopf branch must destabilize before the second connection occurs. This bifurcation is shown in Fig. 5(c), where the optical spectrum is exhibited for $\eta_2 = 0.0355$. Sidebands appear about the two major frequencies of the modes. The frequency of these sidebands corresponds to the relaxation frequency of the laser. However, because the laser is operated at or below a solitary laser threshold, this frequency is close to the external cavity frequency.⁶ The RF spectrum for this case, as shown in Fig. 5(d), supports this interpretation and agrees well with the experimental data.

In summary, we have presented experimental and theoretical observations of dynamic states of a diode laser subject to two sources of delayed optical feedback. These states originate from a novel Hopf bifurcation that involves two distinct ECMs with degenerate intensities. Spectral data show that the sequence of states evolves through stability, periodicity, quasi-periodicity, and the LFF before restabilizing on a new ECM. Experimental and numerical results are in good agreement.

Acknowledgment is made to the W. M. Keck Foundation and the Thomas F. and Kate Miller Jeffress Memorial Trust for the partial support of this research. D. Sukow's e-mail address is sukowd@wlu.edu.

References

1. T. Erneux, F. Rogister, A. Gavrielides, and V. Kovanis, *Opt. Commun.* **183**, 467 (2000).
2. F. Rogister, P. Megret, O. Deparis, M. Blondel, and T. Erneux, *Opt. Lett.* **24**, 1218 (1999).
3. F. Rogister, D. W. Sukow, A. Gavrielides, P. Megret, O. Deparis, and M. Blondel, *Opt. Lett.* **25**, 808 (2000).
4. A. A. Tager and B. B. Elenkrig, *IEEE J. Quantum Electron.* **29**, 2886 (1993).
5. A. A. Tager and K. Petermann, *IEEE J. Quantum Electron.* **30**, 1553 (1994).
6. G. Lythe, T. Erneux, A. Gavrielides, and V. Kovanis, *Phys. Rev. A* **55**, 4443 (1997).